JOURNAL OF VIROLOGY, Oct. 2010, p. 10792–10801 Vol. 84, No. 20
0022-538X/10/$12.00 doi:10.1128/JVI.01168-10

Small Peptide Inhibitors Disrupt a High-Affinity Interaction between Cytoplasmic Dynein and a Viral Cargo Protein▽

Bruno Hernáez,[1] Teresa Tarragó,[2] Ernest Giralt,[2,3] Jose M. Escribano,[1] and Covadonga Alonso[1]*

Instituto Nacional de Investigación y Tecnología Agraria y Alimentaria (INIA), Department of Biotechnology, Autovia A6 Km 7, 28040 Madrid, Spain[1]; Institute for Research in Biomedicine (IRB Barcelona), Barcelona Science Park, Baldiri Reixac 10, E-08028 Barcelona, Spain[2]; and Department of Organic Chemistry, University of Barcelona, Martí i Franquès 1-11, Barcelona, Spain[3]

Received 1 June 2010/Accepted 21 July 2010

Several viruses target the microtubular motor system in early stages of the viral life cycle. African swine fever virus (ASFV) protein p54 hijacks the microtubule-dependent transport by interaction with a dynein light chain (DYNLL1/DLC8). This was shown to be a high-affinity interaction, and the residues gradually disappearing were mapped on DLC8 to define a putative p54 binding surface by nuclear magnetic resonance (NMR) spectroscopy. The potential of short peptides targeting the binding domain to disrupt this high-affinity protein-protein interaction was assayed, and a short peptide sequence was shown to bind and compete with viral protein binding to dynein. Given the complexity and number of proteins involved in cellular transport, the prevention of this viral-DLC8 interaction might not be relevant for successful viral infection. Thus, we tested the capacity of these peptides to interfere with viral infection by disrupting dynein interaction with viral p54. Using this approach, we report on short peptides that inhibit viral growth.

To enter the host cell, a virus must cross several barriers to reach the nucleus. Many viruses hijack the microtubular network to be transported along the cytoplasm (7, 18). Dynein is a microtubular motor protein, part of a large macromolecular complex called the microtubular motor complex. Dynein is involved in early stages of the viral life cycle of diverse infections, the first stage being the intracellular transport of the incoming virus along microtubules. Once transported throughout the cytosol, the virus rapidly gains the perinuclear area or the nucleus, where virus replication takes place. The disruption of microtubules or microtubular motor dynein function impairs the transport of a number of viruses; however, the intrinsic mechanism of this transport is unclear. Also, it has not been firmly established whether there is a common mechanism by which these viruses hijack a component of the microtubular motor complex for this purpose (7). A direct interaction between a given viral protein and cytoplasmic dynein for transport has been reported for HIV, herpes simplex virus, African swine fever virus (ASFV), and rabies virus (4, 14, 22, 25). In adenoviruses, a direct interaction of the viral capsid hexon subunit with cytoplasmic dynein has been described recently (5).

One of these viruses, ASFV, which is a large DNA virus, enters the cell by dynamin- and clathrin-dependent endocytosis (12), and its infectivity is dependent on the acidification of the endosome. ASFV protein p54, a major protein of virion membranes, interacts with the light-chain dynein of 8 kDa (DLC8), which allows the transport of the virus to the perinuclear area (4), in a region called the microtubular organizing center (MTOC). In this zone, the virus starts replication in the viral factory, a secluded compartment where newly formed virions assemble (11, 13). By binding DLC8, the virus masters intracellular transport to ensure successful infection. However, due to the complexity of the system, the mechanism of this interaction is still elusive.

A variety of names have been used for the subunits of the cytoplasmic dynein complex. A new classification for mammalian cytoplasmic dynein subunit genes based on their phylogenetic relationships has been reported in which the DLC8 gene was named DYNLL1 (26).

Light dynein chains are responsible for direct cargo binding in the cell, but how do they select so many different cargos? It is not known whether the mode and site of binding is the same for viral proteins and physiological cargos. Within these multimeric complexes, there are a number of molecules that theoretically could interact with a given viral protein. However, to date viral proteins have been described to bind only light or intermediate dynein chains, such as DLC8 and TcTex1 (4, 5, 8). A candidate viral protein would bind one of the DLC binding domains, which in DLC8 are located between the two dimers of the DLC8 molecule (LysXThrThr). Here, we analyzed this interaction between a viral protein and DLC8 in an attempt to elucidate its requirements and relevance for viral infection.

To determine whether this interaction is crucial for viral replication or whether it is just one of a number of alternatives for the virus-host interplay, we analyzed the capacity of a set of inhibitor peptides targeting a determined binding domain of the DLC8 molecule to interfere with viral infection by disrupting dynein interaction with viral p54.

* Corresponding author. Mailing address: Instituto Nacional de Investigación y Tecnología Agraria y Alimentaria (INIA), Department of Biotechnology, Autovia A6 Km 7, 28040 Madrid, Spain. Phone: 34 91 347 6896. Fax: 34 91 347 8771. E-mail: calonso@inia.es.

▽ Published ahead of print on 4 August 2010.

MATERIALS AND METHODS

Cells and viruses. Vero cells were maintained in Dulbecco's minimum essential medium (DMEM SC; Lonza). In some cases, DMEM SC was supplemented

TABLE 1. Sequence analysis comparison of p54 dynein binding domain from distinct viral isolates

ASFV isolate	Accession no.	Dynein binding sequence in p54[b]	Host	Virulence[a]
BA71V	U18466	HPTEPYTTVTTQNTASQTMS 163	Vero cells	No
Benin 97/1	CAN10225	HPTEPYTTVTTQNTASQTMS 163	Domestic pig	Yes
E75	FJ174394	HPTEPYTTVTTQNTASQTMS 163	Domestic pig	Yes
Coimbra/87	AAY46105	HPTEPYTTVTTQNTASQTMS 163	Domestic pig	NA
Georgia/07	CAQ53724	HPAEPYTTVTTQNTASQTMS 164	Domestic pig	Yes
Ghana/02/1	ACJ61587	HPTEPYTTVTTQNTASQTMS 163	NA	NA
Haiti 81	ACJ37446	HPTEPYTTVTTQNTASQTMS 163	Domestic pig	Yes
Mkuzi/79	ACJ61626	HPTEPYTTVTTQNTASQTMS 163	Ticks	NA
NH/P68	DQ028322	HPTEPYTTVTTQNTASQTMS 150	Domestic pig	No
Nigeria 01	ACJ39045	HPTEPYTTVTTQNTASQTMS 163	Domestic pig	Yes
Pretorisuskop/96/4	AY261363	HPAEPYTTVTTQNTASQTMS 177	NA	Yes
Lillie-148	EU874341	HPAEPYTAVTTQNTASQTMS 169	Domestic pig	Yes
Namibia/Wart80	P0CA00	HPAEPYTTVTTQNTASQTMS 173	Warthog	NA
Lisbon/60	DQ028320	HPTEPYTTVTTQNTASQTMS 163	Domestic pig	Yes
WB87	AY261365	YPAEPYTTVTTQNTASQTMS 175	Ticks	NA
Tengani/62	EU874318	YPAEPYTTVTTQNTASQTMS 175	Domestic pig	Yes
Moz/98/1	ACJ61644	HPAELYTTATTQNTASQTMP 156	NA	NA
Mafra/86	AAY46107	HPTEPYTTVTTQNTASQTMS 163	Domestic pig	NA
Almodóvar/99/NE1	AAY46103	HPTEPYTTVTTQNTASQTMS 163	Domestic pig	NA
Portalegre/90	AAY46109	HPTEPYTTVTTQNTASQTMS 163	Domestic pig	NA
Kenya/50	ACJ61612	PSAELYTTATTQNTASQTMP 155	NA	NA
Malawi LIL 20/1	AY261361	HPAELYTTATTQNTASQTMP 156	Ticks	Yes
Uganda/95/1	ACJ61621	PSDELYTTATTQNTASQTMP 166	Domestic pig	NA

[a] NA, not applicable.
[b] Consensus sequences are underlined.

with 5% inactivated fetal calf serum (Lonza), 4 mM glutamine, 200 IU/ml penicillin, and 100 IU/ml streptomycin (DMEM) (Invitrogen). The BA71V isolate of the African swine fever virus (ASFV) adapted to grow in the Vero cell line (9) was used in the inhibition tests. When indicated, BA71V was purified by ultracentrifugation through a sucrose cushion as previously described (12).

Expression and purification of the recombinant proteins. To obtain the DLC8 spectra by nuclear magnetic resonance (NMR), we used ^{15}N-labeled DLC8 produced in *Escherichia coli*. *E. coli* strain BL21(DE3) previously transformed with vector pET23a-DLC8 (20) was grown in minimal medium including 1% $^{15}NH_4Cl$ (Cambridge Isotope Laboratories) and was induced with 1 mM isopropyl-β-D-thiogalactopyranoside (IPTG) at 30°C for 16 h. The cell pellet then was resuspended in lysis buffer (50 mM Na_2HPO_4, pH 7.0, 300 mM NaCl, 10% glycerol, and anti-proteases [Roche]). After disruption by pulse sonication and incubation with 1 mg/ml lysozyme, histidine-tagged DLC8 was purified by binding to TALON metal affinity agarose (Clontech) after the clearance of cell debris by ultracentrifugation. To prevent precipitation, labeled DLC8 finally was eluted from the column with 200 mM imidazole and dialyzed three times against 1.5 liters of 20 mM ammonium bicarbonate, pH 7.8, and 100 mM NaCl to prevent precipitation. In the case of p54, the corresponding coding sequence from the BA71V isolate lacking the transmembrane domain was cloned into the XhoI site in pET19b (Novagen) to generate pET-p54ΔTM. BL21(DE3) cells transformed with pET-p54ΔTM were grown in LB medium, and protein expression was induced with 1 mM IPTG for 3 h at 37°C. The pellet was resuspended in lysis buffer and disrupted by sonication and lysozyme treatment. His-tagged p54 was purified by binding to TALON, as indicated, and finally eluted in 200 mM imidazole. Protein was dialyzed three times against phosphate-buffered saline (PBS) overnight at 4°C.

NMR spectroscopy. All NMR spectra were recorded on a Bruker spectrometer operating at 600 MHz and equipped with a 5-mm inverse triple-resonance cryogenic probe. Sweep widths of 12 ppm (^{1}H) and 30 ppm (^{15}N), 48 scans, 128 indirect and 2,048 direct data points, and a recycle delay of 1 s were used. A total volume of 160 μl of 0.2 mM DLC8 in 3-mm NMR tubes was used. All DLC8 samples were prepared in 20 mM ammonium bicarbonate and 100 mM NaCl, pH 7.8, in H_2O/D_2O (9:1). To prevent precipitation, p54 was concentrated to 1.5 mM in the same buffer as that used for its purification and then was added to the DLC8 sample. Peptides were dissolved to 25 mM with acetonitrile:H_2O (1:1) and added to the DLC8 sample. All spectra were recorded at 298 K. Spectra processing was performed using TOPSPIN 2.0 software (Bruker).

Peptide compounds. The sequence of p54 in field and laboratory isolates of ASFV deposited in GenBank (NCBI) was plotted into the BLAST database and analyzed with the local alignment search tool. The sequence coding for p54 (E183L gene) is included in the complete sequence of the BA71V isolate, which is deposited in the NCBI database under accession number U18466 (Table 1).

Peptide compound *INTSTP1* (interactionstop1) was designed to contain the DLC8 binding domain found in the ASFV p54 protein. From the sequences flanking the dynein binding domain in different virus isolates we selected those that were more favorable for chemical synthesis. Peptide characteristics are described in Table 2. For this peptide to be used in *in vivo* testing, an arginine tail

TABLE 2. Short peptide sequences designed to compete for p54-cytoplasmic dynein interaction

Peptide	Amino acid (aa) sequence[a]	No. of aa residues	MW[b]	pI	8xR content	FITC[c] label	DLC8 binding domain
INTSTP1	PAEPYTTVTTQNTASQTMS	19	2,028	4	No	No	Yes
INTCT1	SLVSSDESSSGSSHSSGEHS	20	1,949	4.62	No	No	No
INTCT2	RRRRRRRRRSLVSSDESSSGSSHSSGEHS	28	3,199	12	Yes	No	No
DNBLK1	RRRRRRRRRHPAEPGSTVTTQNTASQTMS	28	3,294	12.9	Yes	No	Yes
DNBLK2	RRRRRRRRRHPAEPGSTVTTQNTASQTMS	28	3,653	12.9	Yes	Yes	Yes
DNBLK3	RRRRRRRRRHPTESGSTVTTQNSAAQTMS	28	3,642	12.9	Yes	Yes	Yes
DNBLK4	RRRRRRRRRHPTESGSTVTTQNSASQTMS	28	3,651	12.9	Yes	Yes	Yes

[a] Mutations in the critical binding domain are underlined.
[b] MW, molecular weight.
[c] FITC, fluorescein isothiocyanate.

(8R) was added at the N-terminal end for internalization into cells (peptide *DNBLK1*, for dynblock1) (21). Another series of peptides containing an irrelevant amino acid sequence were synthesized to be used as negative controls (*INTCT1* and *INTCT2* peptides). *INTCT2* was the control sequence, and *INTCT1* plus an octa-arginine tail was used as the control for *in vivo* testing. *DNBLK1* was the original sequence of the dynein binding domain plus the HPAEP flanking sequence, which is similar to that of different virus isolates (Pretorisuskop, Namibia, Lillie-148, Warmbaths WB87, and Tengani isolates) (Tables 1, 2). *DNBLK2* was conjugated to fluorescein at the N-terminal end of *DNBLK1* for its direct visualization with fluorescence microscopy. *DNBLK3* and *DNBLK4* were modified to include conservative artificial point mutations in the binding domain that, not being the original sequence, still retained the ability to bind dynein in the two-hybrid system as described before (4). *DNBLK3* included two point mutations and *DNBLK4* just one point mutation (Table 2). DNBLK3 and DNBLK4 included another flanking sequence, HPTES, which was similar to that of another set of virus isolates, and were conjugated to fluorescein at the N-terminal end for direct visualization with fluorescence microscopy. All of the peptides designed were synthesized by Sigma-Genosys. Purification was carried out by high-performance liquid chromatography (HPLC) to a degree of purity of more than 90%. Once synthesized and purified, lyophilized peptides were received in the laboratory. Depending on their molecular weight (Table 2), the peptides were resuspended in a volume of sterile Milli-Q H_2O to obtain a stock solution at a concentration of 5 mM. Special efforts were made to prevent turbidity in the solution, and filter tips were used to prevent cross-contaminations. Aliquots of 20 μl were made and then conserved at −80°C until use. The working solutions with the peptides were made from the stock solutions in DMEM SC in the 0 to 100 μM range of concentrations prior to addition to the cell culture.

Infectivity assays. Vero cells (9×10^4) were cultured in 24-well plates overnight. The next morning cells were washed in DMEM, and medium was replaced with 300 μl of the solutions containing the peptides at a range of concentrations. Cells were incubated with the peptides for 1 or 3 h at 37°C and 5% CO_2. The medium then was removed and cells were infected with 1 PFU/cell of ASFV strain BA71V. After 2 h at 37°C, residual virus was removed by two washes with DMEM, and finally cells were left in 300 μl of fresh DMEM containing the corresponding peptide concentration. Infection was allowed to proceed at 37°C for the desired time in each experiment, depending on the parameters of the infection to be analyzed.

Indirect immunofluorescence. The detection of cells infected by ASFV in cells previously exposed to the peptides was performed at 6 h postinfection (hpi). Cells were washed with PBS before being fixed with a 3.8% PBS–paraformaldehyde solution at room temperature (RT) for 10 min. After three washes with PBS, cells were permeabilized using 0.2% PBS–Triton X-100 for 15 min at RT. After another three washes with PBS, cells were incubated in blocking solution (3% PBS-bovine serum albumin) at 37°C for 45 min. The detection of the early protein of ASFV p30 (1), the viral antigen chosen for detection, was performed with the anti-p30 antibody (1:200) and incubated for 1 h at 37°C. After three washes in PBS, cells were incubated for 30 min at RT with 1:300 mouse anti-IgG antibody, and nuclei were detected after staining with TO-PRO 3 (Invitrogen). The detection of ASFV virions was performed by incubation with mouse monoclonal antibody anti-p72 clone 1BC11 (Ingenasa) diluted 1:1,000.

Coverslips were mounted with Prolong and observed in a conventional fluorescence microscope (Leica) to count the number of cells positive for the viral antigen p30. Microtubules were detected by staining with anti-α-tubulin monoclonal antibody (Sigma) diluted 1:1,000. A specific rabbit serum against DLC8 was raised after immunization with nonlabeled DLC8 produced in *E. coli*, as described above. This serum was diluted 1:100 in PBS to detect the DLC8 cellular distribution. Anti-mouse IgG or anti-rabbit IgG Alexa 594-conjugated antibodies (Molecular Probes), diluted 1:200 in PBS, were used as secondary antibodies.

Analysis of ASFV proteins by Western blotting. Twenty μg of total soluble protein extracts from Vero cells left unexposed or exposed to the peptides and left uninfected or further infected with ASFV during 16 h were separated by electrophoresis in 15% acrylamide–bisacrylamide gels, and separated proteins were transferred to a nitrocellulose membrane. As primary antibodies, the anti-p30 monoclonal antibody diluted 1:100 in PBS, the anti-p72 monoclonal antibody clone 18BG3 (Ingenasa) diluted 1:2,000 in PBS, and rabbit anti-actin (Sigma) diluted 1:500 were used in independent membranes. ASFV p30 protein is expressed during the initial phases of the infection (1) and p72 protein (also called p73) during the late phase of this process (6, 34). As the secondary antibody, anti-mouse IgG (GE Healthcare) or anti-rabbit IgG (Bio-Rad) conjugated to horseradish peroxidase was used diluted 1:5,000. Finally, bands obtained after development with ECL reagent (GE Healthcare) and corresponding to p30, p72, and β-actin were densitometrically quantified, and data were normalized to control values using a Chemidoc XRS imaging system (Bio-Rad) with Image Lab 2.01 software.

Detection and quantitation of the ASFV genome. The detection and quantitation of the ASFV genome were achieved by quantitative real-time PCR using specific oligonucleotides and a TaqMan probe (16). DNA from infected or mock-infected cells with 0.5 PFU/cell BA71V was extracted and purified with a DNeasy blood and tissue kit (Qiagen) at 16 hpi. DNA concentration and purity was estimated by measuring absorbance at 260 nm (A_{260}). The amplification mixture was prepared on ice as follows: 3 μl template DNA (1 μg), 1 μl oligonucleotide OE3F (50 pmol), 1 μl oligonucleotide OE3R (50 pmol), 10 μl Quantimix easy probes (Biotools) (2×), 1 μl TaqMan probe SE2 (5 pmol), and 4 μl H_2O.

The amplification reaction was performed in a Rotor-Gene RG3000 (Corbett Research) using the following steps: 1 cycle at 94°C for 10 min, 45 cycles at 94°C for 15 s, and 45 cycles at 58°C for 1 min. Positive amplification controls (DNA purified from ASFV virions) and negative amplification controls (DNA from mock-infected cells) were included in the assay, and duplicates from each sample were analyzed.

Effect of peptide treatment on ASFV progeny. Vero cells (9×10^4) were seeded in 24-well plates the night before the experiment. One hour before infection, cells were incubated in 300 μl DMEM containing distinct concentrations of *DNBLK1* and control *INTCT2* peptides. Cells then were mock infected or were infected with 0.5 PFU/cell of ASFV strain BA71V. At 36 hpi, 100 μl of media was collected from wells and stored at −80°C until the analysis of extracellular virus progeny. Infected cells also were collected in 100 μl of fresh DMEM. Cells were frozen and thawed three times to allow the solubilization of intracellular virus progeny and then stored at −80°C until use. Virus titers from intracellular or extracellular samples were analyzed by plaque assay as previously described (13).

Cytotoxicity analysis. Cell viability and proliferation assays. To evaluate cell viability, Vero cells seeded in 24-well plates were incubated in DMEM containing inhibitor *DNBLK1* or negative control *INTCT2* at concentrations ranging from 0 to 100 μM. After incubation with peptides for 24 h, cells were harvested and the number of viable cells in the suspensions was determined by Trypan blue (Sigma) dye exclusion assay. Briefly, 20 μl of PBS with 0.08% Trypan blue was added to an equal volume of cell suspension and mixed. After 2 min, blue cells (dead cells) were counted using a hemocytometer and a conventional light microscope.

To evaluate cell proliferation, 3×10^4 Vero cells seeded in 96-well plates were incubated in 50 μl DMEM containing inhibitor peptide *DNBLK1* or the negative control *INTCT2* at concentrations ranging from 0 to 100 μM. After 36 h of incubation, cell proliferation was determined using the CellTiter 96 Aqueous (Promega) assay by following the manufacturer's instructions.

RESULTS

Sequence analysis comparison of p54 from several viral isolates and peptide design. The minimal region in p54 protein from ASFV isolate BA71V, which maintained DLC8 binding properties, was within a 13-amino-acid fragment between residues 149 and 161 (4). To study the two players in this viral-cellular protein interaction, we started with a comparison analysis of this interacting region in the sequences from several ASFV isolates. This analysis revealed that the DLC8 binding domain in p54 (TVTTQNTASQT) is highly conserved independently of geographic distribution (east and west Africa, Europe, or Central America), year of isolation, host, or virulence status (Table 1). This protein sequence has been extensively studied because of its relevance as a universal diagnostic reagent (3). The coexistence of heterogeneous virus populations in culture-adapted isolates with short amino acid repetitions in p54 without any impact on virus growth was previously described, while no modifications were found in the dynein binding domain (2, 29).

On the basis of this analysis, we designed a set of peptides representing the dynein binding domain and selecting the most favorable flanking sequences, with some variations among isolates. Peptide compound *INTSTP1* (interactionstop1) was de-

signed to contain the DLC8 binding domain found in the ASFV p54 protein. From the sequences flanking the dynein binding domain in different virus isolates we selected those that were more favorable for chemical synthesis. Peptide characteristics are described in Table 2. For this peptide to be used in *in vivo* testing, an arginine tail (8R) was added at the N-terminal end for internalization into cells (*DNBLK1*) (21). Another series of peptides containing an irrelevant amino acid sequence were synthesized to be used as negative controls (*INTCT1* and *INTCT2* peptides). *INTCT2* was the control sequence, and *INTCT1* plus an octa-arginine tail was useful as a control for testing in cells. *DNBLK1* was the original sequence of the dynein binding domain plus HPAEP flanking sequence, which is similar to that of different virus isolates (Pretorisuskop, Namibia, Lillie-148, Warmbaths WB87, Tengani isolates; Tables 1, 2). The following modifications were included: *DNBLK2* was conjugated to fluorescein at the N-terminal end of *DNBLK1* for its direct visualization with fluorescence microscopy. *DNBLK3* and *DNBLK4* were modified to include conservative artificial point mutations in the binding domain that, not being the original sequence, retained the ability to bind dynein in the two-hybrid system as described before (4). *DNBLK3* included two point mutations and *DNBLK4* just one point mutation in the critical amino acid sequence (Table 2). DNBLK3 and DNBLK4 also included another flanking sequence, HPTES, which was similar to that of another set of virus isolates, and were conjugated to fluorescein at the N-terminal end for direct visualization with fluorescence microscopy.

Analysis of the interaction between ASFV protein p54 and dynein light chain by NMR. Nuclear magnetic resonance (NMR) has evolved into a powerful tool for characterizing protein-ligand interactions in solution under near-physiological conditions. Since the natural abundance of one of the most common NMR-observable isotopes, ^{15}N (0.37%), is too low for NMR experiments, the protein to be studied must be isotopically labeled with ^{15}N through expression in *Escherichia coli*. Therefore, all backbone amides as well as the nitrogen-containing side chains are labeled with this magnetically active nucleus. Heteronuclear ^{1}H-^{15}N correlation NMR experiments then can be recorded that generate spectra containing at least one signal for each amino acid, except proline. Additional signals arise from amides in the side chains. When signal assignment is available, a chemical shift perturbation (CSP) experiment enables the mapping of changes in the protein's backbone amides that are induced by the binding of a ligand. (31).

CSP was used to further characterize the p54-DLC8 interaction. First, we obtained an [^{1}H,^{15}N]-HSQC spectrum corresponding to free ^{15}N-labeled DLC8. This spectrum was similar to that previously reported (19) (Fig. 1A). This allowed us to assign most of the signals. We then titrated ^{15}N-labeled DLC8 with a range of concentrations of unlabeled p54 (Fig. 1D). DLC8 resonances progressively disappeared as the p54 concentration increased, thereby suggesting the formation of a higher-molecular-weight complex. Most of the DLC8 resonances were not observable when 2 equivalents (eq) of p54 were added (Fig. 1B). This observation is indicative of a loss of sensitivity as a result of relaxation-dependent line broadening that occurs upon the formation of high-molecular-weight species. As is well known, in large proteins the magnetization relaxes faster, and as a result the peaks become broader and weaker and eventually disappear (35). The first signals to disappear after the addition of 0.1 eq of p54 corresponded to residues W54, I57, K9, Y75, V58, N61, E15, and H68. These residues were mapped on the DLC8 structure (PDB accession number 1PWJ) to define a putative p54 binding surface (Fig. 2).

We then studied the interaction of DLC8 with the peptide *INTSTP1*, which contains the DLC8 binding domain, and an irrelevant amino acid sequence, *INTCT1*, as a control (Table 2). Increasing amounts of both peptides were added to ^{15}N-labeled DLC8, and [^{1}H,^{15}N]-HSQC spectra were recorded. Substantial changes in DLC8 resonances were detected when 5 eq of *INTSTP1* was added (Fig. 1F), while no significant effects were observed with the same amount of *INTCT1* (Fig. 1D). Thus, this observation indicates that *INSTSTP1* bound to DLC8.

Finally, we performed a competition experiment where ^{15}N-labeled DLC8 was incubated with *INTSTP1* before the addition of p54 (Fig. 1C). The binding of p54 to DLC8 was prevented by 5 eq of *INTSTP1*, as indicated by the observation that the higher-molecular-weight complex did not form.

These results confirm the p54-DLC8 interaction and demonstrate that a short peptide containing the minimal DLC8 interaction domain of p54 binds DLC8 *in vitro* and prevents its interaction with p54.

DNBLK peptide is efficiently internalized in Vero cells with no apparent effect on cell proliferation. For this peptide to be used in cells, it must reach the intracellular environment with null or very low toxicity in living cells, and then a guanidinium-rich tail was used to increase cellular uptake. An arginine tail (8R) then was added at the N-terminal end of *INTSTP1* peptide for internalization (*DNBLK1*) (Table 2). To test the intracellular delivery of peptides, we used fluorescein-labeled peptides at the N-terminal end and fluorescence confocal microscopy analysis. *DNBLK2* peptide incorporating the transporter tail was efficiently internalized after 1- and 3-h incubations when the peptide concentration was higher than 25 μM, as almost all of the cells present in the culture incorporated the fluorescent peptide (Fig. 3A). In addition to peptide internalization, we analyzed the integrity of cytoskeletal components. Microtubules were not modified in the presence of any peptide concentration. Also, the DLC8 distribution pattern on microtubules was not modified by the peptide treatment, and DLC8 colocalized to the characteristic condensed perinuclear area corresponding to the MTOC (Fig. 3A).

Dynein function is crucial during mitosis, playing an essential role in the formation of the mitotic spindle and the migration of chromosomes. We studied whether mitosis spindle formation was modified in response to peptide treatment. We found that cell division was not altered (Fig. 3C). Furthermore, the proliferative capacity of the cells was analyzed, measured as the rate of reduction of 3-(4,5-dimethylthiazol-2-yl)-2,5-diphenyltetrasodium bromide (MTT) tetrazolium salt (Fig. 3B). This parameter was not impaired with increasing concentrations of *DNBLK1* compared to the same concentrations of the control peptide *INTCT2* (*INTCT1* plus the intracellular transporter tail) (Table 2). In both cases, the proliferation rates were similar to those obtained for healthy control cells, which

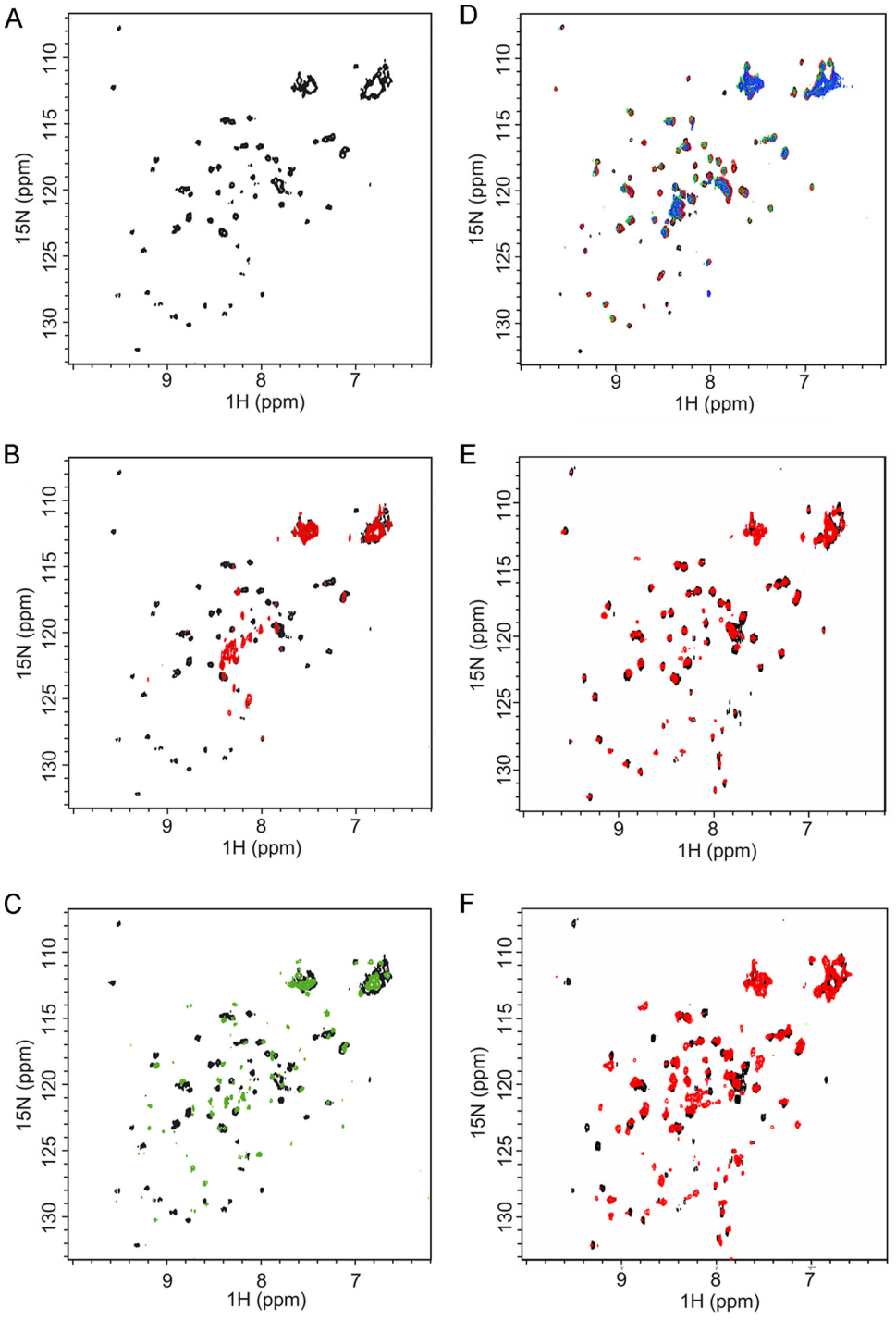

FIG. 1. NMR spectra of free dynein, dynein with the viral protein, and dynein with competitor peptides. NMR spectra of free cytoplasmic dynein compared to that of the protein incubated with increasing concentrations of the viral protein, with or without a competitor peptide, are shown. ^{1}H-^{5}N-HSQC spectra of ^{15}N-labeled DLC8 at several titration points also are shown. In all experiments the observable protein is the ^{15}N-labeled DLC8, as ^{15}N is the NMR-observable isotope. Therefore, we recorded changes in the ^{15}N-labeled DLC8 NMR spectrum after the addition of p54 or the competitor peptides. p54 or the peptides are not observable in these kinds of experiments. The spectra in different colors represent the ^{15}N-labeled DLC8 in different experimental conditions. (A) Free DLC8; (B) free DLC8 (black spectrum) and with 2 eq of unlabeled p54 (red spectrum); (C) free DLC8 (black spectrum) and with 5 eq of peptide *INTSTP1* and 2 eq of unlabeled p54 (green spectrum); (D) free DLC8 (black spectrum) and with 0.1 eq of unlabeled p54 (red spectrum), 0.3 eq of unlabeled p54 (green spectrum), and 0.6 eq of unlabeled p54 (blue spectrum); E, free DLC8 (black spectrum) and with 5 eq of peptide *INTCT1* (red spectrum); (F) free DLC8 (black spectrum) and with 5 eq of peptide *INTSTP1* (red spectrum).

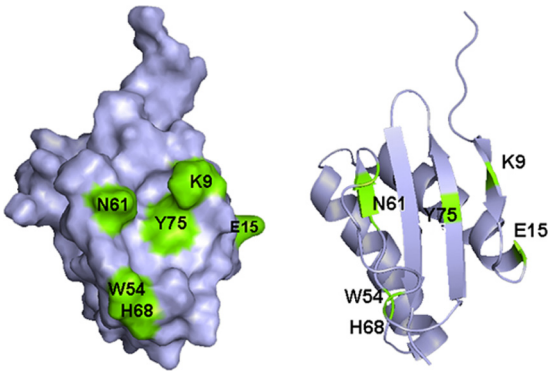

FIG. 2. Mapping of the residues interacting with p54 on the DLC8 surface (PDB accession number 1PWJ). Interacting residues are shown in green.

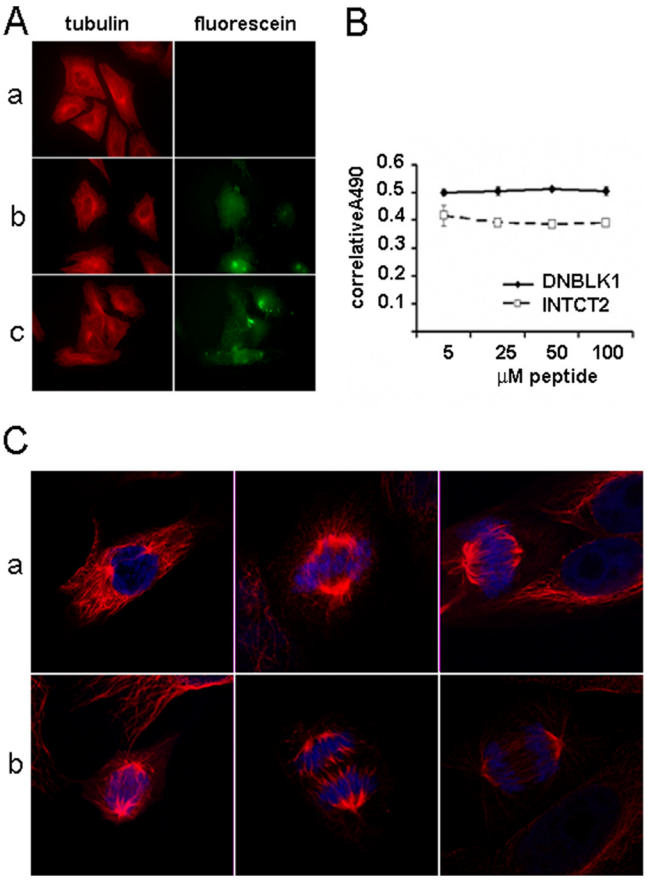

FIG. 3. Cell internalization capacity and cytotoxicity evaluation of selected peptide sequences. (A) Shown are Vero cells treated with increasing concentrations of *DNBLK2* peptide. Competitor peptide sequence is linked to an arginine-rich molecular transporter and labeled with fluorescein. Green fluorescence is observed in cells in which the peptide was successfully internalized. On the left are cells with conserved microtubular cytoskeleton architecture stained with anti-tubulin antibody (red). Note the perinuclear localization of the MTOC. Line a, 5 μM *DNBLK2* peptide; b, 25 μM *DNBLK2* peptide; and c, 50 μM *DNBLK2* peptide. (B) Proliferative index of cells after a 36-h treatment with control *INTCT2* and *DNBLK1* peptides. In both cases, the proliferation rates were similar to those obtained for healthy control cells, 0.4 to 0.5 U. (C) Tubulin fibers forming the mitotic spindle during cell division at different stages in control Vero cells treated with *INTCT2* (a and b) in cells treated with *DNBLK1* peptide. Mitosis morphology and migration along microtubules were not modified by peptide treatment.

was usually 0.4 to 0.5 U. Moreover, no morphological changes indicating cytotoxicity, such as rounding or detaching, were observed in cells incubated with the peptide concentrations for the times assayed.

Effect of DNBLK peptides on ASFV infection. To confirm previous data indicating that microtubules and DLC8 are essential for productive ASFV infection (4), we first analyzed virion distribution by confocal microscopy during the first stages of infection. As expected, we found the association of virions with DLC8 along microtubules (Fig. 4A) immediately after internalization. Figures 4B and C illustrate the early transport of viral particles to the MTOC area from 45 min after infection. ASFV BA71V was used to infect untreated Vero cells or cells treated with *DNBLK1* (Fig. 4C) or with control peptide *INTCT2* (Fig. 4B). At early time points (20 to 45 min after infection), incoming virions were rapidly internalized to the perinuclear area both in untreated and control peptide-treated cells. In the presence of the peptide *DNBLK1*, viral particles remained dispersed in the cytoplasm or in the periphery at the same times.

To evaluate the effect of our set of synthesized peptides on ASFV infection, Vero cells grown to 70% confluence were incubated for 30 min in the absence of fetal bovine serum with increasing concentrations (from 0.5 to 100 μM) of peptides and then infected with approximately 1 PFU/cell of ASFV strain BA71V. Cytopathic effect (CPE), consisting of progressive cell rounding and detachment from the plate surface, is common during ASFV infection. Cells were examined for this effect at 24 hpi. The CPE was dramatically reduced in cells previously incubated with peptides containing the DLC8 binding domain of p54 and also the internalization sequence signal (8xR) (Fig. 4D). However, incubation with the same peptide lacking the internalization signal did not result in CPE abolition, and control peptides (*INTCT2*) yielded the same level of CPE as nontreated cells.

We then analyzed the infectivity of ASFV after incubation with the peptide containing the DLC8 binding domain and internalization signal (*DNBLK1*) by detecting the number of infected cells (Fig. 4E, F). Results showed that the percentage of infected cells detected by indirect immunofluorescence decreased in a dose-dependent manner after incubation with *DNBLK1* but not with control peptides (*INTCT2*). From these experiments, we calculated an EC_{50}, the minimal peptide concentration at which infectivity was inhibited by 50%, of approximately 20 μM.

Also, the synthesis of early (p30) and late (p72) ASFV proteins was analyzed by Western blotting using specific antibodies. The synthesis of early and late viral proteins also decreased in a dose-dependent manner when ASFV infection proceeded in the presence of *DNBLK1* (Fig. 5A), thereby indicating that inhibition mediated by *DNBLK1* occurs early during the ASFV infection cycle.

Similar experiments by quantitative PCR and infectious virus progeny by plaque assay were performed to analyze ASFV replication, as previously described. Levels of ASFV DNA

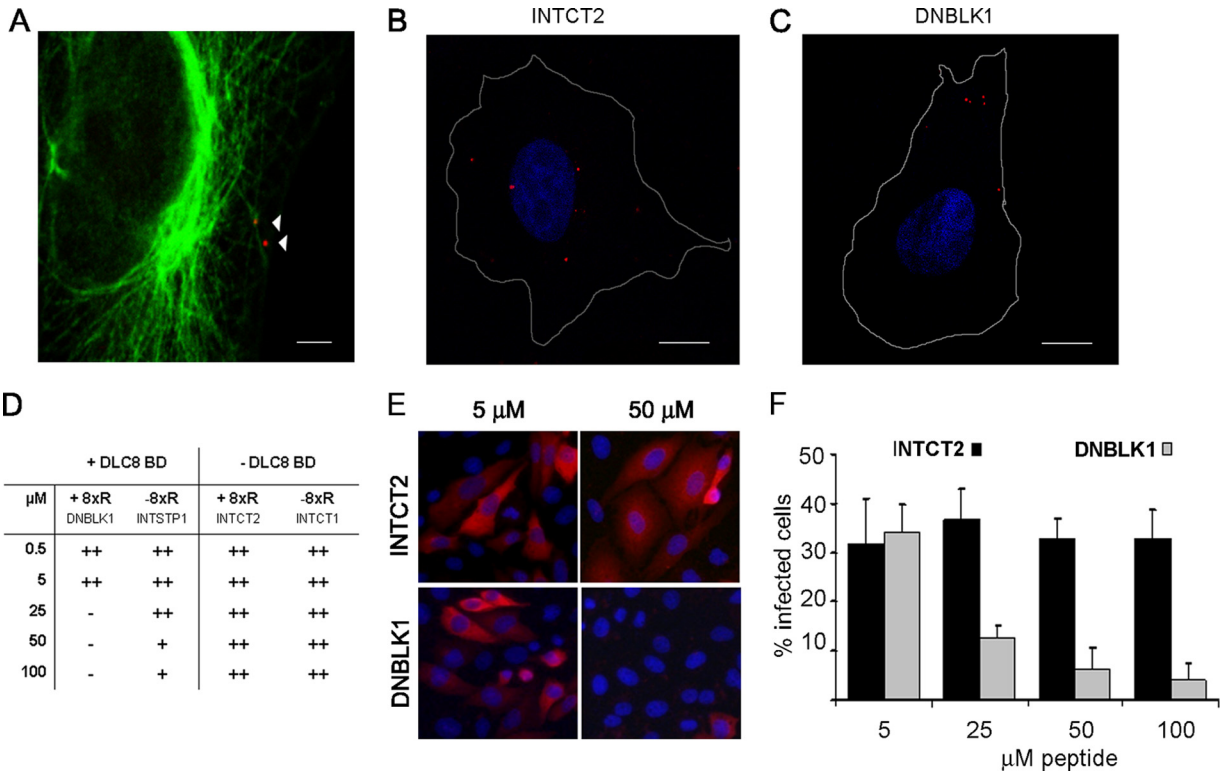

FIG. 4. Decrease of infectivity in cells treated with inhibitor peptide *DNBLK1*. (A) ASFV virions, labeled in red, are transported bound to microtubules by means of p54-microtubular motor dynein interaction. Bar, 2 μm. (B and C) Optical sections (0.1 μm) of Vero cells, 45 min after infection in the presence of 50 μM *INTCT2* or *DNBLK1* peptides, show ASFV virion distribution at early infection stages using a monoclonal antibody against p72 (labeled in red). Nuclei labeled with TO-PRO 3 and cell contour are shown. Bar, 12 μm. (D) Reduction of ASFV cytopathic effect in the presence of increasing concentrations of short peptide sequences designed to compete for the p54-cytoplasmic dynein interaction. Those peptides without an internalization sequence (arginine octapeptide) lack an inhibitory effect. (E) Vero cells incubated with increasing concentrations of inhibitor and control peptides labeled with an antibody against ASFV p30 (in red). (F) Percentages of infected cells at 6 hpi.

were reduced in a dose-dependent manner during infection after incubation with peptides containing the DLC8 binding domain and internalization signal (Fig. 5B). Using this quantitative assay, the peptide *DNBLK1* inhibitory effect was compared to those of two other peptides incorporating point mutations within the dynein binding domain. Those are previously described artificial conservative point mutations that retain the ability to bind dynein assayed by a two-hybrid system (4). *DNBLK3* included two point mutations and *DNBLK4* just one point mutation (underlined in Table 2). Peptide *DNBLK1* showed a greater inhibitory effect than *DNBLK3* and *DNBLK4*, therefore it was selected as the most effective sequence. Nevertheless, control *INTCT2* did not affect normal virus replication. Finally, and to evaluate a possible effect of inhibitory peptides on viral egress, we analyzed intracellular and extracellular virus titers obtained at 36 hpi in the presence of inhibitory and control peptides (Fig. 5C and D). Results showed that both intra- and extracellular virus titers decreased in a dose-dependent way after incubation with *DNBLK1* but not with *INTCT2*.

DISCUSSION

Dynein is a microtubular motor protein responsible for the intracellular transport linked to microtubules. This protein is crucial for the endosomal pathway and organelle intracellular trafficking. In coordination with a number of regulatory molecules, dynein drives motion to regular cargos in the cell (30). Viruses use dynein for their internalization and intracellular transport, as demonstrated for a number of viral models, such as HIV, rabies virus, ASFV, poliovirus, herpes simplex virus, and adenovirus (4, 5, 22, 25, 27). Also, many questions remain unanswered about the intrinsic mechanism of this mode of intracellular transport.

We have analyzed one of the first-described direct interactions between a viral protein and molecular motor dynein for intracellular transport (4). The ASFV protein p54 interacts with DLC8, and this interaction is essential for the intracellular transport of the incoming virus prior to viral protein synthesis and replication in the viral factory, which is located in the perinuclear area in the MTOC, where the new virions are assembled. The p54-dynein interaction was found using the double-hybrid system in yeast, searching for interacting proteins with the viral p54 protein in a swine macrophage cDNA library (4). The clones obtained and identified as positive were sequenced to discover that they contained the complete coding sequence of the light-chain dynein of 8 kDa, named DLC8, LC8, DLC1, or DYNLL1 (26).

Cytoplasmic dynein is a large multimeric complex composed of two heavy chains, a stalk of intermediate chains, and several

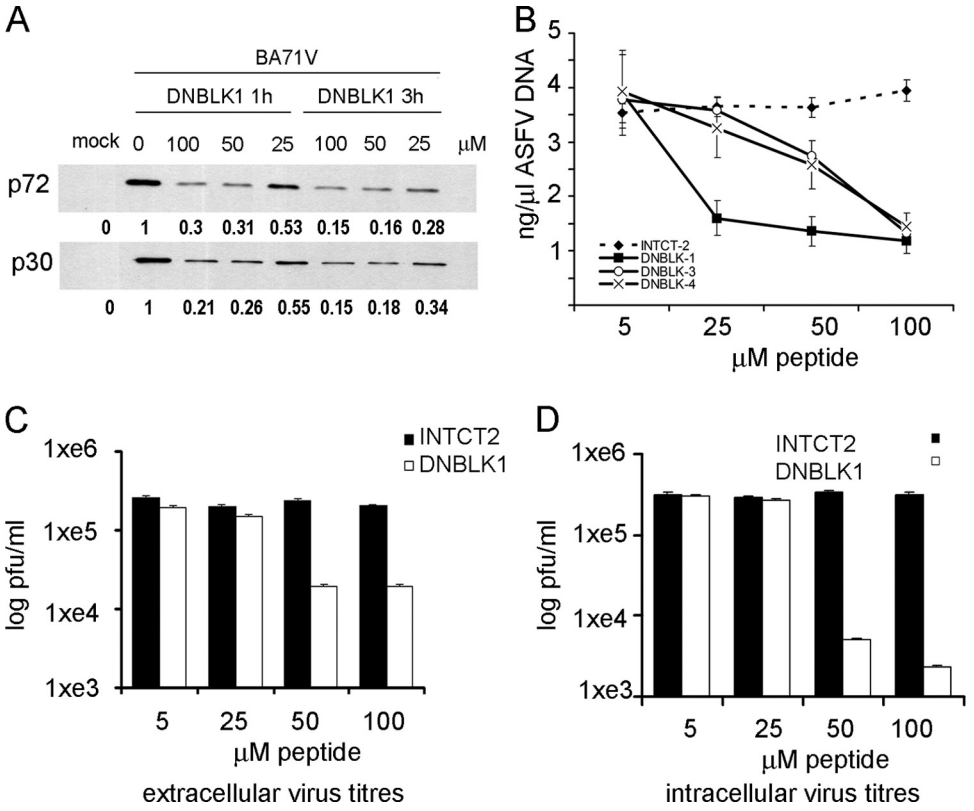

FIG. 5. Effect of peptide pretreatment on viral proteins production, viral replication counts, and total virus production. (A) Western blot analysis of early and late protein synthesis with a range of concentrations of inhibitor and control peptides. The quantification of the intensity of each band is listed under each band. (B) ASFV DNA replication at 16 hpi after treatment with increasing concentrations of inhibitor peptides *DNBLK1*, *DNBLK3*, and *DNBLK4* compared to that of cells treated with control peptide *INTCT2*. The effects on extracellular (C) and intracellular (D) virus titers recovered after 36 hpi with increasing concentrations of inhibitor peptide *DNBLK1* compared to that of the control peptide *INTCT2* are shown.

light chains. Light chains are responsible for a direct interaction with physiological cargos to be transported. Intermediate chains associate with a multisubunit complex, called dynactin, through its projecting arm, named p150-glued. The backbone of this complex is formed by the actin-related protein Arp1 (32). Dynactin is critical in most dynein functions and works as an adaptor connecting to cargo (15). Dynein-driven motion is minus-end directed, but it recently has been shown to direct bidirectional motion to cargos toward both the plus and minus ends of microtubules in diffusive and processive runs (28, 30). The ability of dynein to switch directions increases the flexibility of the system and the capacity to progress around obstacles in a crowded cellular environment.

Several families of dynein light chains have been described among these DLC8 members. There are up to six light chains belonging to three protein families (DYNLL/DLC8, DYNLT/tctex, and DYNLRB/LC7/roadblock), two light intermediate chains (DLIC), and two intermediate chains (DIC), all of which have been implicated in cargo binding (33, 36). DLC8 has a highly conserved nucleotide amino acid sequence between evolutionarily distant species (10, 17).

Regarding the viral interacting protein, the minimal binding domain was identified at the carboxy-terminal end of the protein by expressing several truncated fragments of the p54 protein in the yeast system in 13 amino acids between Tyr149 and Thr161 (TyrThrThrThrValThrThrGlnAsnThrAlaSerGlnThr) (4). Sequence analysis comparison between distinct viral isolates demonstrated that this is a highly conserved sequence among isolates, irrespective of their geographic origin, host, or virulence status. This observation could be attributable to the critical function of this sequence in early infection stages.

The identification of the amino acid sequences involved in the binding between a given viral protein and DLC8 when these sequences are on a primary structure does not necessarily mean that these linear sequences have the capacity to bind or even compete for the binding of the viral protein to DLC8. NMR spectroscopy is a powerful analytical tool to study protein-ligand and protein-protein interaction systems (24, 31). We studied the DLC8-p54 interaction by means of NMR and designed a peptide sequence suitable to target the main residues involved in this binding. CSP analysis showed that DLC8-p54 bound *in vitro* to form a stable-molecular-weight complex. It was found that it was a high-affinity interaction, and the residues gradually disappearing were mapped on DLC8 to define a putative p54 binding surface. A short peptide sequence, containing the DLC8 binding domain, also bound DLC8, and the competition experiments demonstrated that it prevented the binding of the viral protein to DLC8 *in vitro*. This short peptide then was used as a tool to compete with the

viral protein binding to dynein in cells to provide an insight into the result of preventing this single interaction throughout the infection.

In the living cell, however, dynein adaptors and regulators, such as dynactin, help to link dynein to its cargo, and it has been shown that Arp1 and βIII spectrin interaction is sufficient to produce a dynein cargo link (23). In fact, the inhibition of the dynein-dynactin complex by the overexpression of p50 dynamitin blocks ASFV transport in infected cells (4). The p150 subunit also links dynein to cargos, notably through interactions of p150 with regulatory GTPases. Given the complexity and number of proteins involved in cellular transport, the blockage of a determined viral-DLC8 interaction might not suffice to prevent a virus from using the microtubular transport system. Thus, we studied the relevance of this binding for viral infection, and the potential of peptides targeting the binding site was assayed in cells to determine the impact on the viral infection outcome. At micromolar concentrations, a peptide sequence shown to displace and compete with the binding of the viral protein to DLC8 by NMR also was efficient at inhibiting viral infection in susceptible cells. We observed reductions in infectivity, virus replication, and viral production yields. These results highlight the significance of this single interaction and the protein domains involved.

The findings reported here contribute to our understanding of the specificity and relevance of viral strategies evolved to take advantage of cellular transport. In fact, several virus models use dynein for microtubular transport, some of them binding the same DLC8 domain (27). These and other viruses reported to bind dynein for transport are potential candidates for infection inhibition with peptides targeting a crucial step common to many viral infections. Thus, *DNBLK* peptides might be the first clue for the development of an effective treatment against ASFV and other viruses that share the same transport mechanism. Given that viruses are dependent on host cell functions for replication, transient interference with selected interactions of the virus with the cell in which it reproduces may be useful to retard viral replication or spread and, in turn, may spare the host from morbidity or mortality.

ACKNOWLEDGMENTS

We thank Rodriguez-Crespo for the pET23a-DLC8 vector.

This work was supported by grants from the Spanish Ministry of Science and Innovation Program Consolider (CSD2006-00007, PET2006-0785, and BIO2009-09209), Welcome Trust Foundation WT075813, UE project EPIZONE FOOD-CT2006-016236, AGL2007-66441-C03, BIO2008-00799, and the Generalitat de Catalunya (XRB and Grup Consolidat).

REFERENCES

1. **Afonso, C. L., C. Alcaraz, A. Brun, M. D. Sussman, D. V. Onisk, J. M. Escribano, and D. L. Rock.** 1992. Characterization of p30, a highly antigenic membrane and secreted protein of African swine fever virus. Virology **189:** 368–373.
2. **Alcaraz, C., A. Brun, F. Ruiz-Gonzalvo, and J. M. Escribano.** 1992. Cell culture propagation modifies the African swine fever virus replication phenotype in macrophages and generates viral subpopulations differing in protein p54. Virus Res. **23:**173–182.
3. **Alcaraz, C., F. Rodriguez, J. M. Oviedo, A. Eiras, M. De Diego, C. Alonso, and J. M. Escribano.** 1995. Highly specific confirmatory western blot test for African swine fever virus antibody detection using the recombinant virus protein p54. J. Virol. Methods **52:**111–119.
4. **Alonso, C., J. Miskin, B. Hernaez, P. Fernandez-Zapatero, L. Soto, C. Canto, I. Rodriguez-Crespo, L. Dixon, and J. M. Escribano.** 2001. African swine fever virus protein p54 interacts with the microtubular motor complex through direct binding to light-chain dynein. J. Virol. **75:**9819–9827.
5. **Bremner, K. H., J. Scherer, J. Yi, M. Vershinin, S. P. Gross, and R. B. Vallee.** 2009. Adenovirus transport via direct interaction of cytoplasmic dynein with the viral capsid hexon subunit. Cell Host Microbe **6:**523–535.
6. **Cobbold, C., and T. Wileman.** 1998. The major structural protein of African swine fever virus, p73, is packaged into large structures, indicative of viral capsid or matrix precursors, on the endoplasmic reticulum. J. Virol. **72:**5215–5223.
7. **Döhner, K., C. H. Nagel, and B. Sodeik.** 2005. Viral stop-and-go along microtubules: taking a ride with dynein and kinesins. Trends Microbiol. **13:**320–327.
8. **Douglas, M. W., R. J. Diefenbach, F. L. Homa, M. Miranda-Saksena, F. J. Rixon, V. Vittone, K. Byth, and A. L. Cunningham.** 2004. Herpes simplex virus type 1 capsid protein VP26 interacts with dynein light chains RP3 and Tctex1 and plays a role in retrograde cellular transport. J. Biol. Chem. **279:**28522–28530.
9. **Enjuanes, L., A. L. Carrascosa, M. A. Moreno, and E. Vinuela.** 1976. Titration of African swine fever (ASF) virus. J. Gen. Virol. **32:**471–477.
10. **Harrison, A., and S. M. King.** 2000. The molecular anatomy of dynein. Essays Biochem. **35:**75–87.
11. **Heath, C. M., M. Windsor, and T. Wileman.** 2001. Aggresomes resemble sites specialized for virus assembly. J. Cell Biol. **153:**449–455.
12. **Hernaez, B., and C. Alonso.** 2010. Dynamin- and clathrin-dependent endocytosis in African swine fever virus entry. J. Virol. **84:**2100–2109.
13. **Hernaez, B., J. M. Escribano, and C. Alonso.** 2006. Visualization of the African swine fever virus infection in living cells by incorporation into the virus particle of green fluorescent protein-p54 membrane protein chimera. Virology **350:**1–14.
14. **Jacob, Y., H. Badrane, P. E. Ceccaldi, and N. Tordo.** 2000. Cytoplasmic dynein LC8 interacts with lyssavirus phosphoprotein. J. Virol. **74:**10217–10222.
15. **Karki, S., and E. L. Holzbaur.** 1999. Cytoplasmic dynein and dynactin in cell division and intracellular transport. Curr. Opin. Cell Biol. **11:**45–53.
16. **King, D. P., S. M. Reid, G. H. Hutchings, S. S. Grierson, P. J. Wilkinson, L. K. Dixon, A. D. Bastos, and T. W. Drew.** 2003. Development of a TaqMan PCR assay with internal amplification control for the detection of African swine fever virus. J. Virol. Methods **107:**53–61.
17. **King, S. M.** 2003. Organization and regulation of the dynein microtubule motor. Cell Biol. Int. **27:**213–215.
18. **Leopold, P. L., and K. K. Pfister.** 2006. Viral strategies for intracellular trafficking: motors and microtubules. Traffic **7:**516–523.
19. **Lo, K. W., S. Naisbitt, J. S. Fan, M. Sheng, and M. Zhang.** 2001. The 8-kDa dynein light chain binds to its targets via a conserved (K/R)XTQT motif. J. Biol. Chem. **276:**14059–14066.
20. **Martínez-Moreno, M., I. Navarro-Lerida, F. Roncal, J. P. Albar, C. Alonso, F. Gavilanes, and I. Rodriguez-Crespo.** 2003. Recognition of novel viral sequences that associate with the dynein light chain LC8 identified through a pepscan technique. FEBS Lett. **544:**262–267.
21. **Melikov, K., and L. V. Chernomordik.** 2005. Arginine-rich cell penetrating peptides: from endosomal uptake to nuclear delivery. Cell Mol. Life Sci. **62:**2739–2749.
22. **Mueller, S., X. Cao, R. Welker, and E. Wimmer.** 2002. Interaction of the poliovirus receptor CD155 with the dynein light chain Tctex-1 and its implication for poliovirus pathogenesis. J. Biol. Chem. **277:**7897–7904.
23. **Muresan, V., M. C. Stankewich, W. Steffen, J. S. Morrow, E. L. Holzbaur, and B. J. Schnapp.** 2001. Dynactin-dependent, dynein-driven vesicle transport in the absence of membrane proteins: a role for spectrin and acidic phospholipids. Mol. Cell **7:**173–183.
24. **Pellecchia, M., I. Bertini, D. Cowburn, C. Dalvit, E. Giralt, W. Jahnke, T. L. James, S. W. Homans, H. Kessler, C. Luchinat, B. Meyer, H. Oschkinat, J. Peng, H. Schwalbe, and G. Siegal.** 2008. Perspectives on NMR in drug discovery: a technique comes of age. Nat. Rev. Drug Discov. **7:**738–745.
25. **Petit, C., M. L. Giron, J. Tobaly-Tapiero, P. Bittoun, E. Real, Y. Jacob, N. Tordo, H. De The, and A. Saib.** 2003. Targeting of incoming retroviral Gag to the centrosome involves a direct interaction with the dynein light chain 8. J. Cell Sci. **116:**3433–3442.
26. **Pfister, K. K., E. M. Fisher, I. R. Gibbons, T. S. Hays, E. L. Holzbaur, J. R. McIntosh, M. E. Porter, T. A. Schroer, K. T. Vaughan, G. B. Witman, S. M. King, and R. B. Vallee.** 2005. Cytoplasmic dynein nomenclature. J. Cell Biol. **171:**411–413.
27. **Raux, H., A. Flamand, and D. Blondel.** 2000. Interaction of the rabies virus P protein with the LC8 dynein light chain. J. Virol. **74:**10212–10216.
28. **Reck-Peterson, S. L., A. Yildiz, A. P. Carter, A. Gennerich, N. Zhang, and R. D. Vale.** 2006. Single-molecule analysis of dynein processivity and stepping behavior. Cell **126:**335–348.
29. **Rodriguez, F., C. Alcaraz, A. Eiras, R. J. Yanez, J. M. Rodriguez, C. Alonso, J. F. Rodriguez, and J. M. Escribano.** 1994. Characterization and molecular basis of heterogeneity of the African swine fever virus envelope protein p54. J. Virol. **68:**7244–7252.
30. **Ross, J. L., K. Wallace, H. Shuman, Y. E. Goldman, and E. L. Holzbaur.**

2006. Processive bidirectional motion of dynein-dynactin complexes in vitro. Nat. Cell Biol. **8:**562–570.
31. **Salvatella, X., and E. Giralt.** 2003. NMR-based methods and strategies for drug discovery. Chem. Soc Rev. **32:**365–372.
32. **Schroer, T. A.** 2004. Dynactin. Annu. Rev. Cell Dev. Biol. **20:**759–779.
33. **Susalka, S. J., and K. K. Pfister.** 2000. Cytoplasmic dynein subunit heterogeneity: implications for axonal transport. J. Neurocytol. **29:**819–829.
34. **Tabares, E., J. Martinez, F. Ruiz Gonzalvo, and C. Sanchez-Botija.** 1980. Proteins specified by African swine fever virus. II. Analysis of proteins in infected cells and antigenic properties. Arch. Virol. **66:**119–132.
35. **Tugarinov, V., P. M. Hwang, and L. E. Kay.** 2004. Nuclear magnetic resonance spectroscopy of high-molecular-weight proteins. Annu. Rev. Biochem. **73:**107–146.
36. **Vallee, R. B., J. C. Williams, D. Varma, and L. E. Barnhart.** 2004. Dynein: an ancient motor protein involved in multiple modes of transport. J. Neurobiol. **58:**189–200.